Meissner state in finite superconducting cylinders with uniform applied magnetic field

F. M. Araujo-Moreira
Grupo de Supercondutividade e Magnetismo, Departamento de Física, Universidade Federal de São Carlos, Caixa Postal 676, São Carlos SP, 13565-905 Brazil

C. Navau and A. Sanchez
Grup d'Electromagnetisme, Departament de Física, Universitat Autònoma Barcelona, 08193 Bellaterra, Barcelona, Catalonia, Spain
(Received 13 May 1999; revised manuscript received 5 August 1999)

We study the magnetic response of superconductors in the presence of low values of a uniform applied magnetic field. We report measurements of dc magnetization and ac magnetic susceptibility performed on niobium cylinders of different length-to-radius ratios, which show a dramatic enhancement of the initial magnetization for thin samples, due to the demagnetizing effects. The experimental results are analyzed by applying a model that calculates the magnetic response of the superconductor, taking into account the effects of the demagnetizing fields. We use the results of magnetization and current and field distributions of perfectly diamagnetic cylinders to discuss the physics of the demagnetizing effects in the Meissner state of type-II superconductors.

I. INTRODUCTION

Important intrinsic parameters of superconductors, such as the lower critical field H_{c1} and the critical current density J_c, are experimentally obtained by measuring their response to an applied magnetic field. The procedures to obtain these parameters often rely on theoretical approaches developed for infinite samples. When considering realistic finite-size superconductors, important complications arise, so that these methods fail. Even in the case of a uniform field applied to a finite superconductor, in general it is not easy to extract information about the intrinsic parameters of the superconductor since the magnetic response may be strongly dependent on its shape. Demagnetizing effects appearing in finite samples make the internal magnetic field $\mathbf{H}=\mathbf{B}/\mu_0$ in the sample different than the applied one, $\mathbf{H}_a$. The exact relation between both magnetic vectors is in general unknown. As a consequence of this indetermination of the local magnetic field in the sample, the estimations of H_{c1} and other parameters are very complicated. Sometimes this problem is treated by considering a constant demagnetizing factor N, so that the magnetic field in the sample volume $\mathbf{H}$ is assumed to be related to the applied magnetic field $\mathbf{H}_a$ by

$$\mathbf{H}=\mathbf{H}_a-N\mathbf{M}. \tag{1}$$

This procedure is correct only for ellipsoidal-shape samples and when the external magnetic field is parallel to one of its principal axis.[1] In all other cases this equation is not valid and it becomes very hard to find a simple relation between the magnetic vectors $\mathbf{H}$ and $\mathbf{H}_a$. Moreover, in general the field $\mathbf{H}$ is related with $\mathbf{H}_a$ in a different way from point to point in the superconductor.

Recently, there have been important theoretical advances in treating the magnetic response of finite superconducting samples. The magnetic response of finite superconductors in the critical state including demagnetizing effects have been recently calculated for strips[2] and cylinders,[3–5] following previous works on very thin strips[6] and disks.[7] These works deal basically with current and field distributions in superconductors in the mixed state, with critical-state supercurrents penetrating into the bulk of the material. Besides, Chen, Brug, and Goldfarb[1] have calculated demagnetizing factors for cylinders as a function of the length-to-diameter ratio and for different values of the susceptibility χ (including $\chi=-1$).

However, to our knowledge, there has not been done a systematic study involving the comparison between experiments and theoretical data of the Meissner state in superconducting cylinders. This is equivalent to asking which are the currents that completely shield a cylindrical volume and the resulting magnetization.

In this work we systematically investigate the magnetic response of superconducting cylinders in the complete shielding state, by quantitatively studying the effect of demagnetizing fields in their Meissner response. This paper is organized as follows. In Sec. II we discuss the experimental setup and measured samples. In Sec. III we present the experimental results obtained from dc magnetization and ac magnetic susceptibility techniques, performed on niobium cylindrical samples. We introduce in Sec. IV an approach to study the magnetic response of completely diamagnetic finite cylinders. This model allows the interpretation and understanding of our experimental results, which is discussed in Sec. V. The model enables us to calculate the surface current distributions resulting from the magnetic shielding of the cylinder, as well as the magnetic fields created in the exterior of the samples by the induced supercurrents. The results are discussed in Sec. VI. Finally, we summarize our conclusions in Sec. VII.

II. SAMPLES AND EXPERIMENTAL SETUP

We have performed the magnetic characterization of ten cylindrical niobium polycrystalline samples with different values for the ratio L/R, where L and R are the length and

TABLE I. Values of length (L) and radius (R) for the ten Nb samples studied.

Samples	L (mm$\pm$0.01)	R (mm$\pm$0.01)	Measurements
A1	9.72	1.43	ac and dc
A2	1.44	1.43	dc
A3	0.30	1.39	dc
A4	1.38	1.43	ac
A5	0.3	1.43	ac
B1	9.82	1.00	ac and dc
B2	1.50	0.97	dc
B3	0.30	0.96	dc
B4	1.34	0.89	ac
B5	0.44	0.99	ac

the radius of the sample, respectively (see Table I). They were obtained from two different pieces of brut niobium. After machined, they were cleaned in ultrasound bath, and later by using a HCl-HNO_3 solution.

We have studied two families (with five samples in each one) of cylinders with nominal diameters of 1.94 and 2.86 mm, respectively. Samples with the same nominal value for the diameter were cut from the same piece, in cylinders of different lengths. The variation between nominal and real values of the diameter is smaller than 4%.

Before performing magnetic measurements, we have determined the quality of all samples through x-ray diffraction (XRD) and scanning electron microscopy (SEM) analysis. For the XRD we used a Siemens D/5000 diffractometer, and for the SEM, we used a Jeol JSM-5800/LV microscope.

The magnetic characterization was performed through both the magnetization as a function of the external dc magnetic field, $M(H_a)$, and the complex ac magnetic susceptibility, as a function of the absolute temperature $\chi(T)$. To perform those experiments we have used a Quantum Design MPMS5 superconducting quantum interference device magnetometer able to operate in the ranges $2<T<400$ K, $0.1<h<300$ A/m, and $1<f<1000$ Hz, where T, h, and f are the absolute temperature, the amplitude, and the frequency of the ac magnetic field, respectively. In all cases, to avoid trapped magnetic flux, samples were zero-field cooled (ZFC) before each experiment. The magnetic field was always applied along the axis of the cylinders.

III. EXPERIMENTAL RESULTS

The XRD and SEM analysis confirmed the high quality of the niobium samples, as verified by the absence of impurities and the low density of grain boundaries. Measurements of the complex ac magnetic susceptibility, $\chi(T)=\chi'(T)+\chi''(T)$, were performed with the parameters $h=80$ A/m, and $f=100$ Hz, and are shown in Fig. 1. These experiments also confirm the quality of our polycrystals, by showing a critical temperature $T_C=9.2$ K, and sharp superconducting transitions, with typical width of 0.2 K. This value is considered excellent for a polycrystalline sample. These measurements also point out the strong shape effect on $\chi(T)$. As can be seen in Fig. 1, the lower the ratio L/R is, the larger the shape effect is, evidenced for larger values of the modulus of $\chi'(T)$.

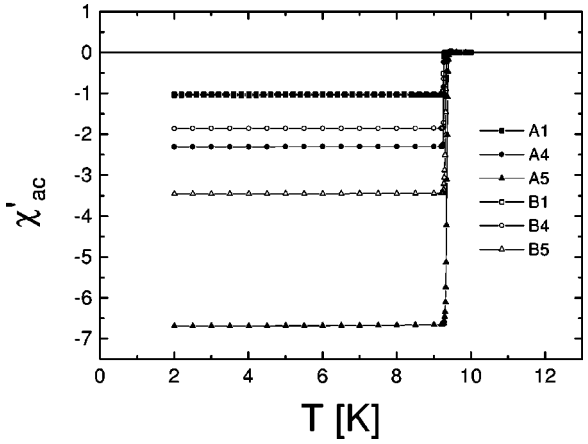

FIG. 1. Real part of the ac magnetic susceptibility as a function of temperature $\chi'(T)$ performed with the parameters $h=80$ A/m, and $f=100$ Hz. Sample identifications are listed in Table I.

As mentioned above, we have also verified the magnetic behavior of the cylinders by measuring isothermal $M(H_a)$ curves. The measurements were performed at $T=8$ K. We show these results in Fig. 2. There we can see again the strong shape effect on the obtained curves. The lower the ratio L/R, the higher the value of the initial slope M/H. Also, we can see the shape effect on the point at which the magnetization curve departs from a straight line, which corresponds to the position where the flux starts to penetrate in the superconductor. Thus flux penetration starts at lower fields for large values of L/R, as expected.

As it was mentioned in the last section, samples with the same nominal diameter were cut from the same piece, in cylinders with different lengths. Since the variation between nominal and real values of the diameter is smaller than 4%, only shape effects will be responsible for the observed difference in their magnetic response.

IV. DESCRIPTION OF THE MODEL

In order to study the Meissner state and analyze the experimental data, we have developed a model to calculate the surface currents that shield any axially symmetric applied magnetic field inside a cylindrical material. This model could

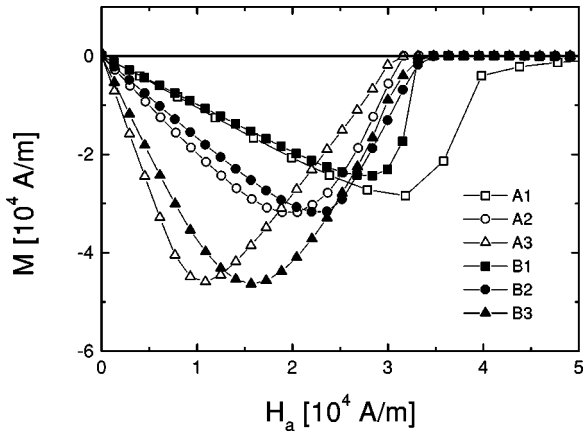

FIG. 2. dc magnetization loops as a function of the applied magnetic field $M(H_a)$ at $T=8$ K. Sample identifications are listed in Table I.

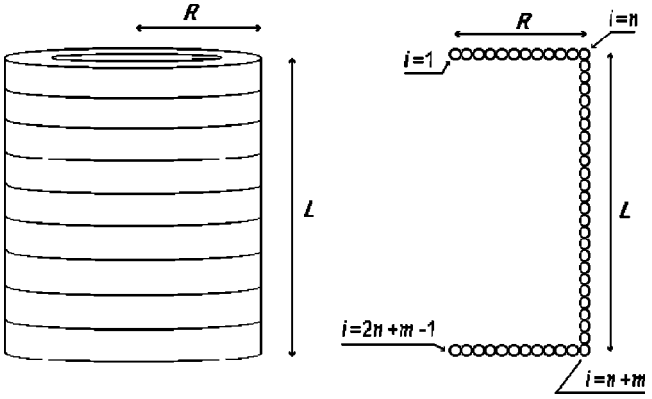

FIG. 3. Sketch of the discretization of the cylinder used in the model.

be applied, in principle, to both type-I and type-II superconductors below H_c and H_{c1}, respectively, and also to good conductors in a high-frequency applied magnetic field.

It is well known that supercurrents are induced in the superconductors in response to variations of the applied magnetic field. For zero-field-cooled type-II superconductors in the Meissner state, in order to minimize the magnetic energy, these supercurrents completely shield the applied magnetic field inside the superconductor. This shielding occurs over the whole sample volume except for a thin surface shell of thickness λ (the London penetration depth), where supercurrents flow. Our model simulates this process. It will enable us to calculate the current distribution that shields the applied magnetic field, by finding at the currents that minimize the magnetic energy in the system. For simplicity, we will assume that λ is negligible. In this approximation, the calculated supercurrents flow only in the cylinder surfaces.

We consider a cylindrical type-II superconductor of radius R and length L with its axis in the z direction, in the presence of a uniform applied magnetic field $\mathbf{H_a}=H_a\hat{\mathbf{z}}$. We use cylindrical coordinates (ρ,φ,z). Owing to the symmetry of the problem all shielding currents will have azimuthal direction. We divide the superconducting cylinder surfaces into a series of concentric circular circuits in which currents can flow, with no limitation in the value of current. We consider n of such circuits in each one of the cylinder's ends and m circuits in the lateral surface (see Fig. 3). These linear circuits are indexed, as seen in Fig. 3, from $i=1$ to $i=2n+m-1$.

The method to obtain the current profile is the following. We start with a zero-field-cooled (ZFC) superconductor and set an applied field H_a. The magnetic flux that threads the area closed by the i circuit due to the external field is

$$\Phi_i^a=\mu_0\pi\rho_i^2H_a, \tag{2}$$

ρ_i being the radius of the i circuit. The magnetic flux contributes with an energy that has to be counteracted by induced surface currents. A step of current ΔI that is set in some j circuit requires an energy

$$E_j=\frac{1}{2}L_j(\Delta I)^2, \tag{3}$$

L_j being the self-inductance of the j circuit, while it contributes to reduce the energy by a factor $(\Delta I)\Phi_j^a$. So, after an external field is applied, we seek for the circuit that decreases the energy the most and set a current step ΔI there. The same criterion is used next to choose either to increase the current at the same circuit by another step ΔI, or instead put ΔI at some new circuit. In the last case (and in the general case when they are curents circulating in many circuits of the sample), the energy cost to set a current step has an extra term coming from the mutual inductances of all other currents:

$$E_j=\left(\sum_{k\neq j}M_{kj}I_k\right)\Delta I_j. \tag{4}$$

The mutual inductances M_{ij} between the i and j linear circuits are calculated using the Neumann formulas (see, for example, Ref. 8). To avoid diverging self-inductances, we have used a cutoff and calculated the self-inductance of a circuit with radius ρ from the mutual inductance between the considered circuit and one with the same current at a radial position $\rho+\epsilon$. An appropriate choice for ϵ has been found to be $\epsilon=0.78\Delta R$, where ΔR is the radial separation between two consecutive circuits in the end faces ($\Delta R=R/n$).

The minimun energy corresponding to a given value of the applied magnetic field will be reached when it becomes impossible to further decrease the magnetic energy by setting extra current steps. From the existing current profile, we can easily obtain the different magnitudes we are interested in. The magnetization, which has only axial direction M_z, is calculated by using

$$M_z=\frac{1}{R^2L}\sum_i I_i\rho_i^2. \tag{5}$$

The magnetic induction **B** could be computed from the current profiles using the Biot-Savart formulas. However, we use a simpler way, which allows the calculation of **B** from the flux. In our model, the total magnetic flux that threads any circular circuit (not necessarily those in the surfaces of the superconductor) can be easily calculated as

$$\Phi(\rho,z)=\Phi^a(\rho,z)+\Phi^i(\rho,z), \tag{6}$$

where the internal flux that threads a j circuit due to all the currents is $\Phi_j^i=\Sigma_kM_{jk}I_k$ (the term of the self-inductances is also included). Then, the axial component of the total magnetic induction is simply

$$B_z(\rho,z)=\frac{\Phi(\rho+\Delta R,z)-\Phi(\rho,z)}{\pi[(\rho+\Delta R)^2-\rho^2]}. \tag{7}$$

The radial component $B_r(\rho,z)$ is calculated from the values of the axial one, imposing the condition that the divergence of **B** equals zero.

Finally, if the external magnetic field is further increased, the same procedure starts again from the present distribution of current.

The values of n and m have been chosen sufficiently large so that the results are independent of their particular value. Typical values are $n\cdot m\sim 7500$–$10\,000$. The computation

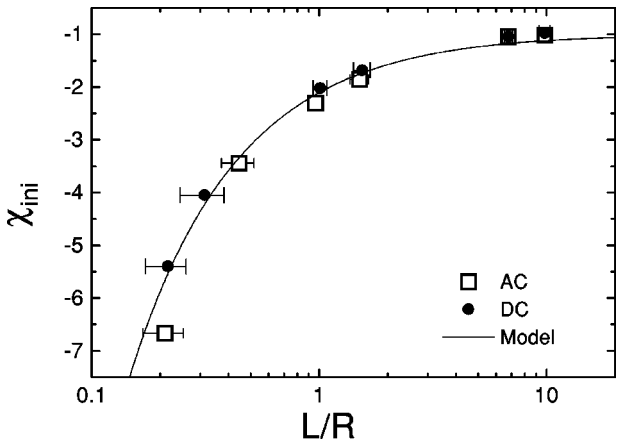

FIG. 4. Initial susceptibility for diamagnetic cylinders of radius R and length L as a function of L/R. Squares and circles are experimental data from ac and dc experiments performed on niobium cylinders, respectively. The line corresponds to our model calculation. Vertical error bars are smaller than symbol size.

time for an initial curve in a personal Digital Workstation takes few minutes for any L/R ratio.

We would like to remark that, with the method described here, we obtain the current distribution, field profiles, magnetization, and all the other results without using any free parameter. Only the direction of currents has to be known, which is straightforward in this geometry.

V. COMPARISON OF EXPERIMENTAL AND THEORETICAL DATA

In Fig. 4 we compare the experimental values of the initial magnetic susceptibility $\chi_{\rm ini}$ obtained from both dc and ac measurements, with those calculated from our model, for different values of L/R. The calculated values of the initial slope are only function of the length-to-radius ratio L/R. The agreement with the experimental data is then very satisfactory, confirming the validity of our theoretical approach. Both experimental and calculated data indicate a strong increase in the absolute value of the initial susceptibility when decreasing the cylinder aspect ratio. When the sample is very large (for $L>10R$), the initial susceptibility $\chi_{\rm ini}$ approaches the value predicted for infinite samples, $\chi_{\rm ini}=-1$. For shorter samples, the magnetization gets larger in magnitude for the same value of the applied magnetic field. We find that the general behavior of the dependence of $\chi_{\rm ini}$ on L/R is well described (with a departure of less than 1.5% from our calculations) by the approximate formula given by Brandt:[3]

$$\chi=-\pi R^2 L-\frac{8}{3}R^3-\frac{4R^3}{3}\tanh\left[1.27\frac{L}{2R}\ln\left(1+\frac{2R}{L}\right)\right]. \tag{8}$$

The values of the initial slope calculated from our model are also compatible with those given by Chen, Brug, and Goldfarb[1] for cylinders with $\chi=-1$ with a maximum deviation of 1.0%.

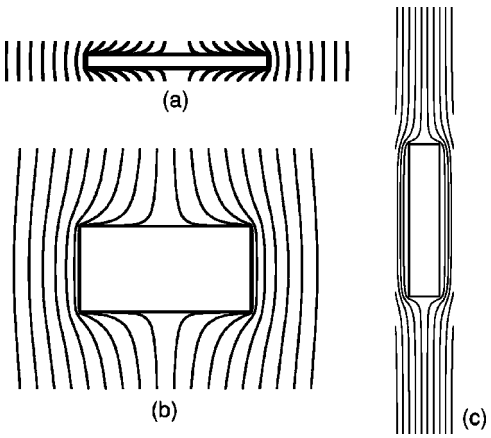

FIG. 5. Theoretical sketch of the total magnetic field lines **B** for three diamagnetic cylinders with length-to-radius ratios $L/R=$ (a) 0.2, (b) 1, and (c) 10. The lines describe the field direction at every point, but the field strength is not given by the density of lines.

VI. DISCUSSION

A. Effect of the demagnetizing fields

The experimental and theoretical results can be understood from analyzing the effect of the demagnetizing fields. In an unrealistic infinitely long sample, if the field is applied along its axis, shielding currents will flow only in the lateral surface, with a constant value along the cylinder. This creates a spatially uniform magnetic field over the superconductor, which makes $\mathbf{B}=0$ inside. In finite samples, however, in the top and bottom end surfaces the tangential magnetic field is not continuous and shielding currents are also there induced. Hence these currents create an extra nonuniform magnetic field over the lateral surface of the cylinder, so the currents flowing in this surface will not have a constant value. It is easily seen (by a simple examination of the magnetic field created by each single current loop) that the effect that the demagnetizing fields produce in the lateral surface region is to enhance the local magnetic field. In this case, its total value is larger than the actual value of H_a. As a result, higher values of current are necessary to shield the applied magnetic field, yielding to larger values of both the magnetization and the magnetic susceptibility. It is clear that the thinner the sample is, the larger this effect occurs, which explains the increase of $|\chi|$ when decreasing L/R.

B. Field and current profiles

The previous discussions can be illustrated by studying the distribution of the magnetic field in finite cylinders. In Fig. 5 we show the calculated total magnetic induction **B** for cylinders with three different values of L/R. The displayed lines indicate the direction of **B** (tangential to the lines at each point), although their densities do not reflect in general the field strength. These results show that only in the case of the largest L/R ratio the magnetic field in the lateral surface can be considered as basically having a constant (axial) direction over the cylinder length. In the other two cases, the magnetic field loses its main axial direction, gradually bending towards the axis at both cylinder ends.

In Fig. 6 we plot the calculated surface current density corresponding to the $L/R=1$ case. In both top and bottom

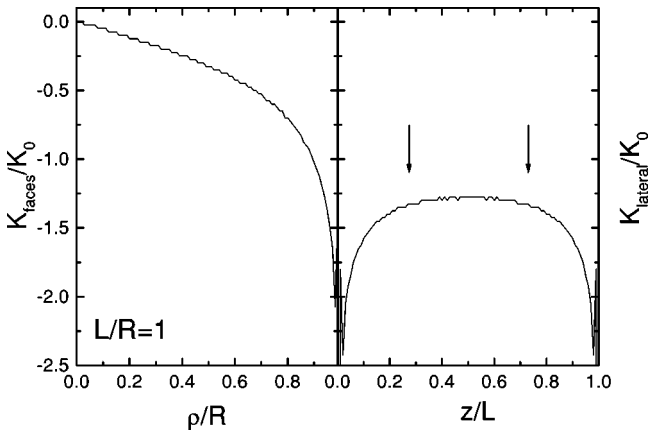

FIG. 6. Theoretical values of the surface shielding current K for the case $L/R=1$, as a function of radial and axial positions ρ and z, respectively. K is normalized to the value K_0 defined as the surface current value that would shield the same applied field H_a for an infinite sample, that is, $K_0=H_a$. The left part of the figure corresponds to the current in the end surfaces of the cylinder K_{faces} and the right one to the current in the lateral surface K_{lateral}. The arrows mark the plateau of almost costant current (see text).

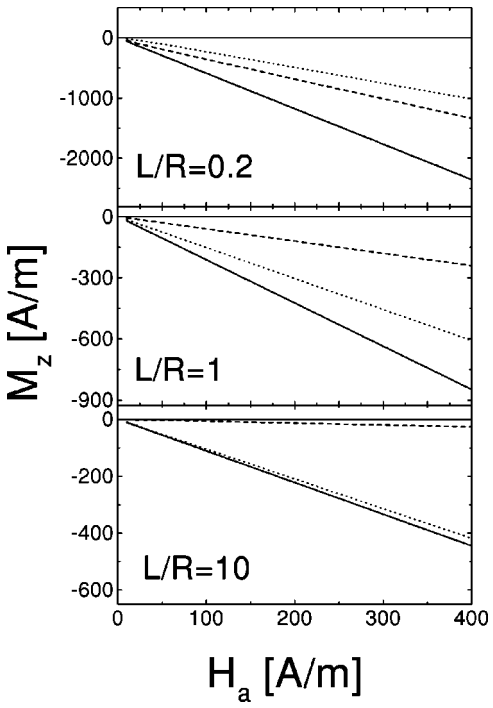

FIG. 7. Theoretical contribution from the lateral and end surfaces of diamagnetic cylinders to the magnetization, for the cases $L/R=0.2$, 1, and 10. Dotted, dashed, and solid lines correspond to the contribution from the lateral surface, the contribution from the end surfaces, and the total, respectively.

ends of the cylinder, the strength of the shielding supercurrents flowing in the azimuthal direction gradually grows (in absolute value) from a zero value over the axis to a diverging behavior when reaching the cylinder edge (this divergence is smoothed because of our discretization; in actual experiments the nonzero value of λ makes also smooth values). The currents in the lateral surface are also stronger at the edges and their intensity decrease towards the center of the sample, where they have a roughly constant value over the plateau shown in Fig. 6. The extension of this plateau (if defined as the region where the surface current differs less than 5% with respect to the minimum value, located at the center) is of about 70% of the total cylinder length, for $L/R=10$. This percentage decreases to 46 and 36% for $L/R=1$ and $L/R=0.2$, respectively (for clarity, Fig. 6 does not show the data for the cases $L/R=0.2$ and 10). This is in correspondence with the regions, shown in Fig. 5, where the magnetic field is almost constant. Besides, our calculations show that the relative contribution of the currents in the end surfaces to the magnetization increases by decreasing the cylinder thickness. The contributions of the lateral and the end surfaces to the total magnetization are depicted in Fig. 7. These results show that, whereas in a long sample ($L/R=10$) about 94% of the contribution to the superconductor magnetization comes from the lateral surface, this percentage decreases to about 72 and 43%, for $L/R=1$ and $L/R=0.2$, respectively.

C. Remarks about the generality of the results

In the $M(H_a)$ experimental data, Fig. 2, the curves for different L/R show a systematic behavior in the first portion of the initial curve (region of interest). There the shielding should be perfect. Nevertheless, the trend is not so clear for larger values of the applied magnetic field. In the middle part of the loop, it is known that bulk supercurrents penetrate into the superconductor, which goes from the Meissner state to the mixed state. Within the critical-state model framework, the magnetization in the mixed state is known to be dependent on the particular $J_c(B)$ dependence of the samples.[9] This depends itself on factors such as the detailed microstructure of the sample. Thus samples with different microstructures may have a difference distribution of pinning strengths and locations, which influences the critical current and the magnetization. The samples we have measured were cut from two different cylinders, which explains why the $M(H_a)$ loops for intermediate values of H_a are different. The systematic behavior observed in the initial susceptibility despite using samples from different original pieces, supports the generality of our results for any diamagnetic cylinder.

VII. CONCLUSIONS

In this work we propose a model based on energy minimization which allows the calculation of the magnetic response for perfectly diamagnetic cylinders of any size with high precision. The only assumption we have considered is that the magnetic penetration depth λ is negligible. We have experimentally verified the validity of this model by measuring the low-field magnetic response of niobium cylinders with different values for the length-to-radius ratio. We have demonstrated both experimentally and theoretically that the value of the initial susceptibility of zero-field-cooled type-II superconductor cylinders is a function of only the sample aspect ratio, and calculated its value for a wide range of

sample dimensions. The model is sufficiently general to be adapted to other geometries and also to nonuniform axially symmetric applied fields. These results may help to discriminate whether some of the effects recently observed in the study of thin-film high-T_c superconductors are due to intrinsic causes or instead have an extrinsic origin associated with sample size effects.

ACKNOWLEDGMENTS

We thank DGES Project No. PB96-1143 for financial support. C.N. acknowledges a grant from CUR (Generalitat de Catalunya). F.M.A.M. gratefully acknowledges financial support from Brazilian agencies CNPq and FAPESP, through Grant Nos. 98/12809-7 and 99/04393-8.

[1] D.-X. Chen, J.A. Brug, and R.B. Goldfarb, IEEE Trans. Magn. **27**, 3601 (1991).

[2] E.H. Brandt, Phys. Rev. B **54**, 4246 (1996).

[3] E.H. Brandt, Phys. Rev. B **58**, 6506 (1998).

[4] T.B. Doyle, R. Labusch, and R.A. Doyle, Physica C **290**, 148 (1997).

[5] A. Sanchez and C. Navau, IEEE Trans. Appl. Supercond. **9**, 2195 (1999).

[6] E.H. Brandt, M. Indenbom, and A. Forkl, Europhys. Lett. **22**, 735 (1993); M. Darwin, J. Deak, L. Hou, M. McElfresh, E. Zeldov, J.R. Clem, and M. Indenbom, Phys. Rev. B **48**, 13 192 (1993).

[7] P.N. Mikheenko and Y.E. Kuzovlev, Physica C **204**, 229 (1993); J. Zhu, J. Mester, J. Lockhart, and J. Turneaure, *ibid.* **212**, 216 (1993); J.R. Clem and A. Sanchez, Phys. Rev. B **50**, 9355 (1994).

[8] J.D. Jackson, *Classical Electrodynamics* (Wiley, New York, 1975), p. 262.

[9] D.-X. Chen and R.B. Goldfarb, J. Appl. Phys. **66**, 2489 (1989); D.-X. Chen, A. Sanchez, and J.S. Muñoz, *ibid.* **67**, 3430 (1990); D.-X. Chen, A. Sanchez, J. Nogués, and J.S. Muñoz, Phys. Rev. B **41**, 9510 (1990).